inorganic compounds

Sr–fresnoite determined from synchrotron X-ray powder diffraction data

Anthony M. T. Bell[a]* and C. Michael B. Henderson[b]

[a]HASYLAB/DESY, Notkestrasse 85, 22607 Hamburg, Germany, and [b]School of Earth, Atmospheric and Environmental Sciences, University of Manchester, Manchester, M13 9PL, England
Correspondence e-mail: tony.bell@desy.de

The fresnoite-type compound $Sr_2TiO(Si_2O_7)$, distrontium oxidotitanium disilicate, has been prepared by high-temperature solid-state synthesis. The results of a Rietveld refinement study, based on high-resolution synchrotron X-ray powder diffraction data, show that the title compound crystallizes in the space group $P4bm$ and adopts the structure of other fresnoite-type mineral samples with general formula $A_2TiO(Si_2O_7)$ (A = alkaline earth metal cation). The structure consists of titanosilicate layers composed of corner-sharing SiO_4 tetrahedra (forming Si_2O_7 disilicate units) and TiO_5 square-based pyramids. These layers extend parallel to the ab plane and are stacked along the c axis. Layers of distorted SrO_6 octahedra lie between the titanosilicate layers. The Sr^{2+} ion, the SiO_4 tetrahedron and the bridging O atom of the disilicate unit are located on mirror planes whereas the TiO_5 square-based pyramid is located on a fourfold rotation axis.

Related literature

For the crystal chemistry of fresnoites, see: Barbar & Roy (2012); Höche *et al.* (2002); ICDD (1989). For properties of Sr–fresnoites, see: Park & Navrotsky (2010). Atomic coordinates as starting parameters for the Rietveld refinement (Rietveld, 1969) of the present phases were taken from Ochi (2006); Goldschmidt & Thomassen (1923); Machida *et al.* (1982); Mitchell *et al.* (2000). For related strontium titanosilicates, see: Miyajima *et al.* (2002). For synchrotron data analysis, see: Hammersley (1997); Hammersley *et al.* (1996).

Experimental

Crystal data

$Sr_2TiSi_2O_8$	Z = 2
M_r = 407.31	Synchrotron radiation,
Tetragonal, $P4bm$	λ = 0.207549 Å
a = 8.3200 (3) Å	μ = 0.43 mm^{-1}
c = 5.0239 (2) Å	T = 293 K
V = 347.77 (2) Å^3	Cylinder, 20 × 0.7 mm

Data collection

In-house design diffractometer	Scan method: continuous
Specimen mounting: capillary	$2\theta_{min}$ = 0.053°, $2\theta_{max}$ = 11.915°,
Data collection mode: transmission	$2\theta_{step}$ = 0.008°

Refinement

R_p = 0.052	χ^2 = 31.068
R_{wp} = 0.073	1476 data points
R_{exp} = 0.031	71 parameters
R_{Bragg} = 0.093	5 restraints

Data collection: local software; cell refinement: local software; data reduction: local software; program(s) used to solve structure: coordinates taken from a related compound; program(s) used to refine structure: *FULLPROF* (Rodriguez-Carvajal, 2001); molecular graphics: *VESTA* (Momma & Izumi, 2008); software used to prepare material for publication: *publCIF* (Westrip, 2010).

Supplementary data and figures for this paper are available from the IUCr electronic archives (Reference: WM2699).

References

Barbar, S. K. & Roy, M. (2012). *J. Therm. Anal. Calorim.* doi:10.1007/s10973-012-2336-0.
Goldschmidt, V. M. & Thomassen, L. (1923). *Skr. Nor. Vidensk. Akad. Oslo*, **5**, 1–48.
Hammersley, A. P. (1997). ESRF Internal Report No. ESRF97HA02T. ESRF, Grenoble, France.
Hammersley, A. P., Svensson, S. O., Hanfland, M., Fitch, A. N. & Häusermann, D. (1996). *High Pressure Res.* **14**, 235–248.
Höche, T., Neumann, W., Esmaeilzadeh, S., Uecker, R., Lentzen, M. & Rüssel, C. (2002). *J. Solid State Chem.* **166**, 15–23.
ICDD (1989). *PCPDFWIN*. International Centre for Diffraction Data, Newtown Square, Pennsylvania, USA.
Machida, K.-I., Adachi, G.-Y., Shiokawa, J., Shimada, M. & Koizumi, M. (1982). *Acta Cryst.* B**38**, 386–389.
Mitchell, R. H., Chakhmouradian, A. R. & Woodward, P. M. (2000). *Phys. Chem. Miner.* **27**, 583–589.
Miyajima, H., Miyawaki, R. & Ito, K. (2002). *Eur. J. Mineral.* **14**, 1119–1128.
Momma, K. & Izumi, F. (2008). *J. Appl. Cryst.* **41**, 653–658.
Ochi, Y. (2006). *Mater. Res. Bull.*, **41**, 740–750.
Park, T.-J. & Navrotsky, A. (2010). *J. Am. Ceram. Soc.* **93**, 2055–2061.
Rietveld, H. M. (1969). *J. Appl. Cryst.* **2**, 65–71.
Rodriguez-Carvajal, J. (2001). URL: http://www.ill.eu/sites/fullprof/
Westrip, S. P. (2010). *J. Appl. Cryst.* **43**, 920–925.

supporting information

Sr–fresnoite determined from synchrotron X-ray powder diffraction data

Anthony M. T. Bell and C. Michael B. Henderson

S1. Comment

The title compiound, $Sr_2TiO(Si_2O_7)$, is the Sr analogue of the mineral fresnoite, $Ba_2TiO(Si_2O_7)$. It is of interest as a potential storage medium for radioactive strontium from nuclear waste (Park & Navrotsky, 2010). An incommensurately modulated structure of Sr-fresnoite has been determined from room-temperature single crystal data and refined in the 5D superspace group $P4bm$ (-α, α, 1/2; α, α, 1/2) with α = 0.3 and with lattice parameters a = 8.312 (2) Å and c = 10.07 (1) Å (Höche *et al.*, 2002). However, ICDD PDF card 39–228 (ICDD, 1989) states that at room temperature this material is tetragonal with space group $P4bm$ and lattice parameters a = 8.3218 (2) Å and c = 5.0292 (2) Å. The crystal structure of the mineral fresnoite has been decribed in the same space group with lattice parameters a = 8.5159 (6) Å and c = 5.2184 (4) Å. Solid solutions with composition $Ba_{2-x}Ca_xTiO(Si_2O_7)$ (x = 0.0, 0.2, 0.4, 0.8, 1.0; Barbar & Roy, 2012) adopt the same structure. The ordered crystal structure of $Sr_2TiO(Si_2O_7)$ in space group $P4bm$ and a halved c parameter in comparison with the single crystal study is reported in the present communication.

The mean Si—O and Ti—O distances in the titanosilicate layer of Sr-fresnoite are respectively 1.64 Å and 1.92 Å. The corresponding Si—O and Ti—O distances are 1.64 Å and 1.93 Å in fresnoite. The respective distances in the structures of the solid solutions $Ba_{2-x}Ca_xTiO(Si_2O_7)$ are: 1.59 Å and 2.01 Å (x = 0.2); 1.65 Å and 2.03 Å (x = 0.4); 1.66 Å and 2.02 Å (x = 0.8); 1.71 Å and 1.95 Å (x = 1.0) (Barbar & Roy, 2012). Due to the distortion of the crystal structures by the partial replacement of Ba by Ca these distances are less comparible with those in Sr-fresnoite.

The mean Sr—O distance in the title structure is 2.62 Å, which is comparible with the mean Sr—O distance of 2.61 Å in $Sr_4Ti_5O_8(Si_2O_7)_2$ (Miyajima *et al.*, 2002).

The O—Si—O angles deviate significantly from the ideal tetrahedral angle of 109.5°, indicating a strong distortion due to the presence of the TiO_5 polyhedra in the titanosilicate layer.

Fig. 1 shows the Rietveld difference plot for the present refinement. The crystal structure of $Sr_2TiO(Si_2O_7)$ is displayed in Fig. 2 and consists of layers of corner-sharing SiO_4 and TiO_5 polyhedra extending parallel to the *ab* plane. These layers are separated along the *c* axis by layers of distorted SrO_6 octahedra.

S2. Experimental

A synthetic sample of Sr-fresnoite was made by melting a stoichiometric mixture of $SrCO_3$, TiO_2 and SiO_2 to form a glass. This glass was then quenched to 293 K, reground and then heated for 7 days at 1323 K. A small amount of CeO_2 (*NIST* SRM 674*a*) standard was added to this powdered sample to act as an internal standard.

S3. Refinement

The powdered sample was loaded into a 0.7 mm diameter quartz capillary, prior to synchrotron X-ray powder diffraction data collection using the P02.1 high resolution powder diffraction beamline at the PETRA-III synchrotron. The beam on the sample was 0.8 mm wide and 1.27 mm high. Powder diffraction data were collected using a PerkinElmer XRD 1621

flat panel image plate detector, which was approximately 1.4 m from the sample. One powder diffraction dataset was collected at 293 K out to approx. 11.9°/2θ, the data collection time was 30 s. Powder diffraction data were converted to a list of 2θ and intensity using FIT2D (Hammersley *et al.*, 1996, Hammersley, 1997). Powder diffraction data in the range 1–11.7°/2θ were used for the Rietveld refinement. Data below 1°/2θ were excluded due to scatter from the beam stop and as there were no Bragg reflections in this region. Data above 11.7°/2θ were excluded as this corresponded to the edge of the image plate detector where the Bragg peaks were weaker.

The main Bragg reflections of the powder diffraction pattern could be indexed in space group *P4bm* with similar lattice parameters to those of PDF card 39–228 (ICDD, 1989). The unit cell of the incommensurately modulated structure (Höche *et al.*, 2002) corresponds to a doubled *c* axis compared to that given on the PDF card. The doubled *c* axis does not match with some of the low-angle Bragg reflections for the $Sr_2TiO(Si_2O_7)$ sample used in the present study, therefore this incommensurate structure was not used for Rietveld refinement. Bragg reflections for three impurity phases could also be identified in the powder diffraction data. $SrTiO_3$ and $SrSiO_3$ were formed as by-products during preparation.

Initial lattice parameters for the three Sr-containing phases were refined using local software. The CeO_2 (*NIST* SRM 674*a*) standard was used to calibrate the sample to detector distance. The CeO_2 lattice parameter was fixed at 5.4111 Å so as to calibrate the wavelength as 0.207549 Å.

The *P4bm* crystal structure of the mineral fresnoite ($Ba_2TiO(Si_2O_7)$; Ochi, 2006) was used as a starting model for the Rietveld refinement (Rietveld, 1969) of the structure of $Sr_2TiO(Si_2O_7)$. The crystal structures of $SrSiO_3$ (Machida *et al.*, 1982), $SrTiO_3$ (Mitchell *et al.*, 2000) and CeO_2 (Goldschmidt & Thomassen, 1923) were used for the impurity phases in the refinement. Isotropic atomic displacement parameters were used for all phases. For the $Sr_2TiO(Si_2O_7)$ phase the Si—O and Ti—O distances in the SiO_4 and TiO_5 polyhedra were soft-constrained to those for $Ba_2TiO(Si_2O_7)$ (Ochi, 2006). The U_{iso} factors for all O sites were constrained to be the same. 81 (1) wt.% of Sr-fresnoite was present in this sample with 4.6 (3) wt.% CeO_2, 7.0 (6) wt.% $SrTiO_3$ and 7.4 (8) wt.% of $SrSiO_3$ present as impurities.
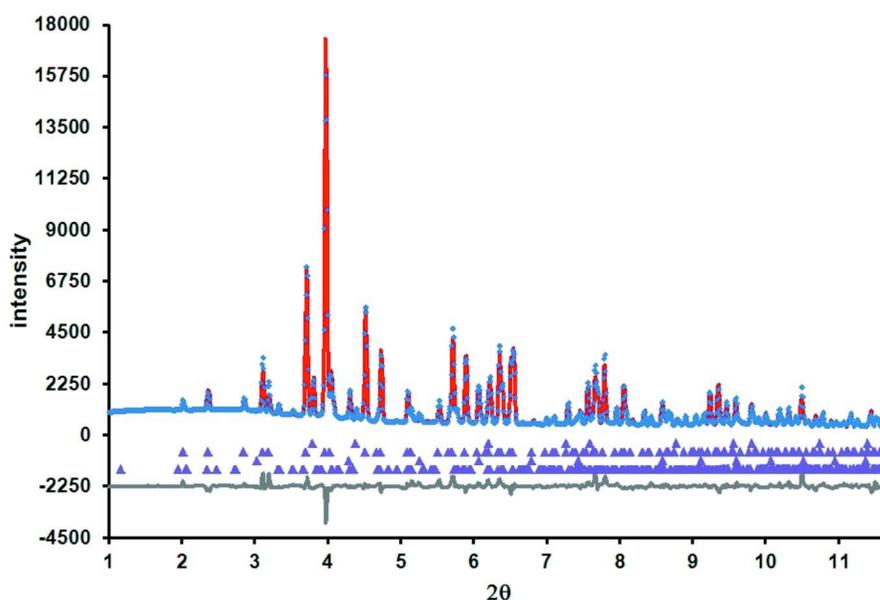
Figure 1

Rietveld difference plot for the multi-phase refinement of $Sr_2TiO(Si_2O_7)$, CeO_2, $SrTiO_3$ and $SrSiO_3$. The blue crosses, and red and black lines show respectively the observed, calculated and difference plots. Calculated Bragg reflection positions are indicated by triangles for the four phases.
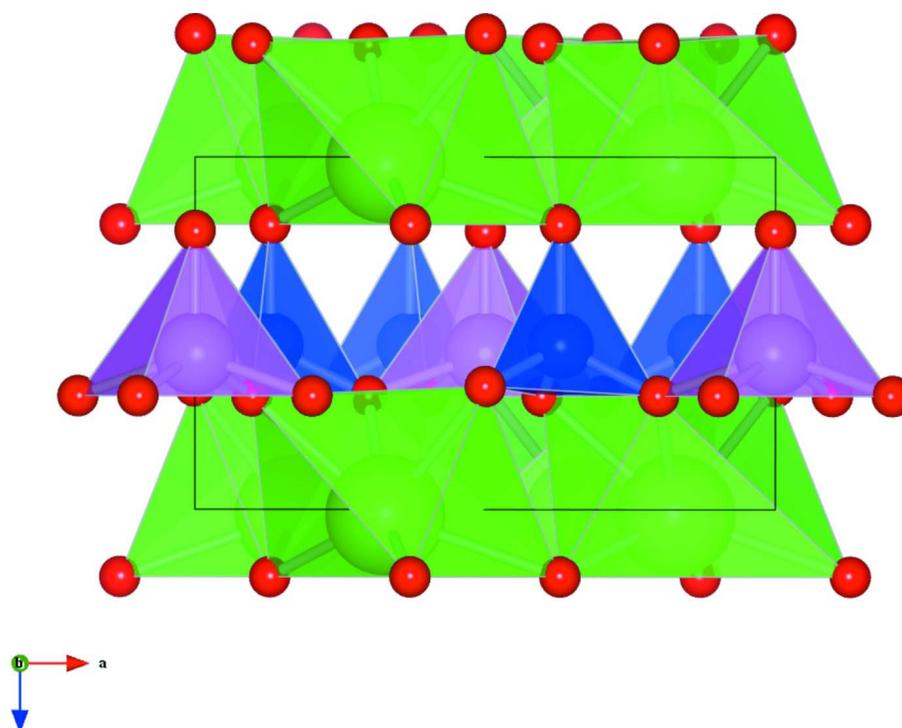
Figure 2

The crystal structure of $Sr_2TiO(Si_2O_7)$. Purple polyhedra show TiO_5 units, blue polyhedra show SiO_4 units, green polyhedra show distorted SrO_6 units. Green spheres represent Sr atoms, pink spheres represent Ti atoms, blue spheres represent Si atoms and red spheres represent O atoms.

Distrontium oxidotitanium disilicate

Crystal data

$Sr_2TiSi_2O_8$	Synchrotron radiation, $\lambda = 0.207549$ Å
$M_r = 407.31$	$\mu = 0.43$ mm^{-1}
Tetragonal, $P4bm$	$T = 293$ K
Hall symbol: P 4 -2ab	Particle morphology: powder
$a = 8.3200\ (3)$ Å	white
$c = 5.0239\ (2)$ Å	cylinder, 20×0.7 mm
$V = 347.77\ (2)$ Å^3	Specimen preparation: Prepared at 1323 K and
$Z = 2$	100 kPa
$D_x = 3.890\ (1)$ Mg m^{-3}	

Data collection

In-house design diffractometer	Specimen mounting: capillary
Radiation source: Synchrotron	Data collection mode: transmission
Laue DCM diamond(111) & Si(111) monochromator	Scan method: continuous
	$2\theta_{min} = 0.053°$, $2\theta_{max} = 11.915°$, $2\theta_{step} = 0.008°$

Refinement

$R_p = 0.052$	$R_{Bragg} = 0.093$
$R_{wp} = 0.073$	1476 data points
$R_{exp} = 0.031$	

Excluded region(s): 0–1 and 11.7–12.0 degrees 2θ	71 parameters
	5 restraints

Profile function: T-C-H Pseudo-Voigt function

Fractional atomic coordinates and isotropic or equivalent isotropic displacement parameters ($Å^2$)

	x	*y*	*z*	U_{iso}*/U_{eq}
Sr1	0.3282 (2)	0.8282 (2)	0.017 (2)	0.0070 (8)*
Ti1	0.00000	0.00000	0.558 (3)	0.007 (2)*
Si1	0.1305 (6)	0.6305 (6)	0.535 (3)	0.019 (2)*
O1	0.00000	0.50000	0.651 (5)	0.017 (3)*
O2	0.1292 (15)	0.6292 (15)	0.191 (3)	0.017 (3)*
O3	0.2985 (12)	0.5984 (15)	0.678 (3)	0.017 (3)*
O4	0.00000	0.00000	0.209 (3)	0.017 (3)*

Geometric parameters (Å, º)

Sr1—O1[i]	2.733 (18)	Ti1—O3[viii]	1.961 (12)
Sr1—O2	2.499 (13)	Ti1—O3[ix]	1.961 (13)
Sr1—O2[ii]	2.676 (13)	Ti1—O4	1.75 (2)
Sr1—O2[iii]	2.676 (13)	Si1—O1	1.642 (11)
Sr1—O3[iv]	2.572 (15)	Si1—O2	1.73 (2)
Sr1—O3[v]	2.572 (14)	Si1—O3	1.594 (14)
Ti1—O3[vi]	1.961 (12)	Si1—O3[x]	1.594 (15)
Ti1—O3[vii]	1.961 (13)		
O3[xi]—Ti1[xii]—O3[xiii]	84.6 (9)	O3[x]—Ti1[xii]—O4[xii]	107.9 (12)
O3[xi]—Ti1[xii]—O3[xiv]	144.2 (10)	O3[xiv]—Ti1[xii]—O4[xii]	107.9 (12)
O3[xiv]—Ti1[xii]—O3[xiii]	84.6 (8)	O1—Si1—O2	110.3 (16)
O3[xi]—Ti1[xii]—O4[xii]	107.9 (12)	O1—Si1—O3[x]	108.0 (9)
O3[xiv]—Ti1[xii]—O3[x]	84.6 (8)	O1—Si1—O3	108.0 (10)
O3[xiii]—Ti1[xii]—O3[x]	144.2 (11)	O2—Si1—O3	117.1 (15)
O3[xiii]—Ti1[xii]—O4[xii]	107.9 (12)	O2—Si1—O3[x]	117.1 (15)
O3[x]—Ti1[xii]—O3[xi]	84.6 (9)	O3[x]—Si1—O3	95.2 (11)

Symmetry codes: (i) −*y*+1, *x*+1, *z*−1; (ii) −*y*+1, *x*+1, *z*; (iii) *y*, −*x*+1, *z*; (iv) *x*, *y*, *z*−1; (v) *y*−1/2, *x*+1/2, *z*−1; (vi) −*x*+1/2, *y*−1/2, *z*; (vii) *y*−1/2, *x*−1/2, *z*; (viii) *x*−1/2, −*y*+1/2, *z*; (ix) −*y*+1/2, −*x*+1/2, *z*; (x) *y*−1/2, *x*+1/2, *z*; (xi) −*x*+1/2, *y*+1/2, *z*; (xii) *x*, *y*+1, *z*; (xiii) −*y*+1/2, −*x*+3/2, *z*; (xiv) *x*−1/2, −*y*+3/2, *z*.